Prospective results of CHANG'E-2 X-ray spectrometer

PENG Wen-Xi(彭文溪) WANG Huan-Yu(王焕玉)[1)] ZHANG Cheng-Mo(张承模)
CUI Xing-Zhu(崔兴柱) CAO Xue-Lei(曹学蕾) ZHANG Jia-Yu(张家宇) LIANG Xiao-Hua(梁晓华)
WANG Jin-Zhou(汪锦洲) GAO Min(高旻) YANG Jia-Wei(杨家卫) WU Ming-Ye(吴明烨)

(Institute of High Energy Physics, CAS, Beijing 100049, China)

Abstract The Chinese second lunar satellite CE-2, which carries an X-ray spectrometer (XRS), will be launched at the end of 2010. In order to estimate the scientific results of XRS, we simulate the anticipated lunar X-ray spectra observed by XRS by using the expected mean solar X-ray flux in 2011. We also obtain the integration time and the spatial resolution required to achieve a certain significance level for the major lunar rock-forming elements in different solar activity conditions. It is expected that a spatial resolution of finer than 100 kilometers can be achieved for elements Mg, Al, Si, Ca, Ti, and Fe.

Key words moon, X-ray fluorescence, solar cycle

PACS 96.20.-n, 95.85.Nv

1 Preface

Remote X-ray spectrometry is a key technique in measuring the lunar chemical composition. Since it is too cool to emit any X-rays by itself, the X-ray emission from the Moon's surface is excited by solar X-ray photons[1—4]. When the solar X-rays interact with the atoms at the uppermost layer of the Moon's, corresponding characteristic X-ray fluorescence will be produced if the energy of the incident X-ray emission exceeds the binding energy of the inner-shell (K or L) electrons of these atoms[1—3]. In addition, coherently and incoherently scattered X-rays, which constitute the continuous component of the lunar X-ray emission, are also produced from the lunar surface. Analyzing the X-ray spectrum collected with a detector orbiting around the Moon, we can obtain the elemental composition and distribution of the lunar surface. Table 1 shows the K-line emission properties of the major elements on the Moon[4].

The solar X-ray flux is known to vary with time[1]. Actually, the variations of solar X-ray irradiation correlate with the 11-year solar activity cycle. During the time around the solar activity minimum, the Sun can remain quiescent without any flare occurrence for weeks, and the solar X-ray emission has the lowest flux, about 10^{-8} W/m^2 (GOES A-level[2)]). At the solar maximum, the occurrence rate of flares, especially

Table 1. The characteristic lines of rock-forming elements on the Moon.

elements	atomic No.	Kα_1/keV	relative intensity	Kα_2/keV	relative intensity	Kβ/keV	relative intensity
O	8	0.525	100	0.525	50	—	—
Mg	12	1.253	100	1.253	50	1.302	1.9
Al	13	1.487	100	1.486	50	1.557	2.8
Si	14	1.740	100	1.739	50	1.836	8.8
Ca	20	3.692	100	3.688	50.2	4.013	19.2
Ti	22	4.511	100	4.505	50.3	4.932	20.1
Fe	26	6.404	100	6.391	50.6	7.058	20.3

Received 6 January 2009, Revised 25 March 2009

1) E-mail: wanghy@mail.ihep.ac.cn

2) Solar X-ray flux levels are classified as A, B, C, M and X according to the 1—8Å flux measured by the GOES satellite. Each class has a flux ten times greater than the preceding one, and Class A has a flux of the order 10^{-8} W/m^2. Solar X-ray flares use the peak flux for classification.

that of large solar flares, strongly increases, and the solar background X-ray flux is usually elevated by several orders of magnitude from the solar minimum to the solar maximum[5].

The increased solar X-ray flux (1—10 keV) will largely enhance the intensity of lunar X-ray fluorescence, particularly the fluorescent lines of heavy elements (e.g., Ti, and Fe). As a result, the occasion of remote X-ray observation is crucial and the perfect observing time should be close to the solar maximum.

2 X-ray spectrometer onboard CE-2

The first Chinese lunar satellite CHANG'E-1 (CE-1) ended its life by impacting the Moon on March 1st, 2009. During its more than one year lifetime, the XRS[6] (Fig. 1) onboard CE-1 successfully detected the characteristic X-ray fluorescent lines emitted from the lunar rock-forming elements, such as Mg, Al, and Si[7, 8]. Unfortunately, 2008 was the solar minimum year in solar cycle 23, which means that the solar X-ray flux was the lowest. Accordingly, the lunar fluorescent X-rays excited by the solar X-rays were so few that the elemental abundance distribution could hardly be obtained.

However, the second Chinese lunar satellite CE-2 is under manufacture and the launch time is around 2011. CE-2 is almost the twin of CE-1, and no significant difference exists between them except the orbit. The orbital altitude of CE-2 will be 100 km and be kept for only 6 months. A new version of the X-ray spectrometer (XRS) will be carried by CE-2 and a ^{55}Fe source will be added on the XRS to calibrate its in-orbit performance. The characteristics of the XRS are listed in Table 2. Compared with the XRS onboard CE-1, only the lower limit of the energy range of the Hard X-ray Detector (HXD) is changed from 10 keV to 25 keV to lower the electronic noise of the detectors.

Table 2. Performance of the XRS onboard CE-2.

total mass 5.5 kg total power 23.6 W			
components	soft X-ray detector (SXD)	hard X-ray detector (HXD)	solar X-ray monitor (SXM)
objects	lunar X-ray fluorescence	natural radiation from the Moon	solar X-ray
detector	Si-PIN×4 chips	Si-PIN×16 chips	Si-PIN×1 chips
filter	12.5 μm beryllium	1 μm aluminum	12.5 μm beryllium
energy range	0.5—10 keV	25—60 keV	0.5—10 keV
effective area	1 cm^2	16 cm^2	0.75 mm^2
energy resolution	300 eV@5.9 keV	6 keV@5.9 keV	300 eV@5.9 keV
ADC	10 bits	10 bits	10 bits

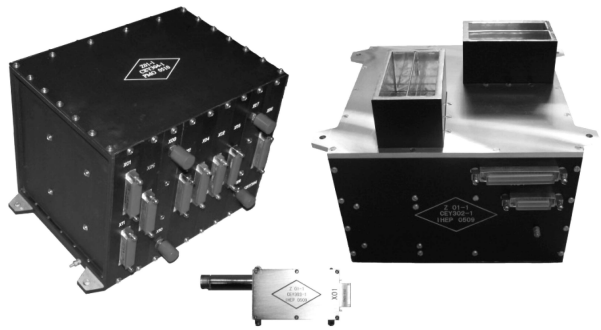

Fig. 1. Photographs of the X-ray spectrometer. Left: electronic box; middle: solar X-ray monitor; right: lunar X-ray detector.

The mission time in 2011 will be excellent for XRS to perform remote lunar X-ray observation as the solar maximum will be approaching. Even so, it is still necessary to estimate the anticipated results of XRS before launching. Therefore, in this article, we first estimate the solar X-ray output level in 2011 based on the prediction of the solar activities; then we build a theoretical lunar X-ray production model for XRS to calculate the anticipated lunar X-ray spectra and the achievable spatial resolutions for the major elements on the Moon. We only focus on the calculation for the SXD units which measure the lunar X-ray fluorescence.

3 The solar activity in 2011

Before calculating the X-ray spectrum of the Moon's surface obtained by XRS, we need to know the solar X-ray output level in 2011. As mentioned above, the output of solar irradiation strongly depends on the solar activities. Therefore, first, we focus on estimating the solar activity in 2011, which is based on the prediction of the next solar cycle: solar cycle 24.

The solar cycle, i.e. the sunspot cycle, first drew

scientists' attention due to the discovery of the periodic variation of the monthly mean sunspot number (Fig. 2). According to statistical data, the sunspot number R is closely related to the other solar activity indicators[9—11], thus the prediction of solar activity generally is focused on studying the variation of R, especially its amplitude (maximum sunspot number) and peak time.

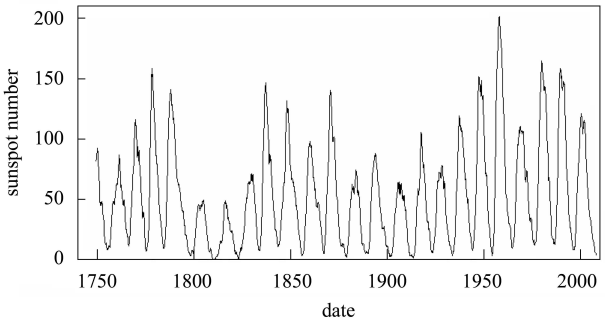

Fig. 2. Smoothed monthly sunspot number since 1749[10].

Actually, predicting the solar cycle is quite difficult, partly because the features of the solar cycle, such as amplitude, shape and duration, vary from cycle to cycle[12]; and partly because the knowledge of the solar cycle mechanism is still poor (the famous solar dynamo model, which gives a good explanation about the origin of solar cycle[13, 14], has been well developed in the past few decades but needs further improvement to interpret all the phenomena in the solar cycle[10]). Even so, several tens of methods are used to forecast the properties of solar cycle 24[10, 15]. The most widely used prediction was released by the Solar Cycle 24 Prediction Panel[1)] on April 25, 2007[10]. According to this prediction, the monthly sunspot numbers of the year 2011, represented as R_2011, are expected to reach 70±10 in a weak cycle or 125±20 in a strong cycle.

On the other hand, the relationship between the sunspot number and the solar X-ray background flux can be used to estimate the mean output of solar X-rays in 2011. Fig. 3 shows the scatter plot of the smoothed monthly solar X-ray background fluxes based on GOES data versus the sunspot numbers (data from the Sunspot Index Data Center) in solar cycle 23, which can be fitted by a power-law[11]

$$Y = AX^B \ , \qquad (1)$$

where X denotes the sunspot numbers, Y denotes the smoothed monthly solar X-ray background flux, A and B are the constant coefficients.

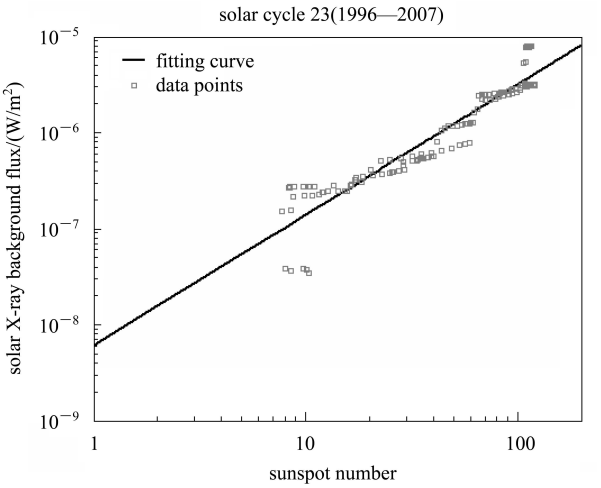

Fig. 3. Scatter plots of the smoothed monthly solar X-ray background fluxes against the sunspot numbers for solar cycle 23 (1996—2008).

The linear fit in log-log space yields $\log_{10} A = -8.21 \pm 0.07$, $B = 1.36 \pm 0.04$ and the correlation coefficient $r = 0.94$. If X is set to R_2011 in Eq. (1), we obtain an estimate of the solar X-ray background flux in 2011 (Table 3).

Table 3. The expected solar X-ray background flux in 2011.

X=R_2011	solar X-ray background flux/(W/m^2)
70±10	(1.99±0.61)×10^{-6}
125±20	(4.38±1.39)×10^{-6}

In addition, we plot the smoothed monthly solar X-ray flare numbers versus the sunspot numbers for solar cycles 21—23 (1975—2008) in Fig. 4. Eq. (1) is also used for fitting but Y denotes the smoothed monthly numbers of solar X-ray flares here.

According to the fitting results shown in Table 4, the occurrence rates of various solar X-ray flares in 2011 are calculated and listed in Table 5.

Table 4. Fitting results using Eq. (1). (X: sunspot numbers, Y: the smoothed monthly numbers of solar X-ray flares).

flare class	lg A	lg A error	B	B error	r
$\geqslant C1$ & $< M1$	−0.41	0.04	1.29	0.02	0.95
$\geqslant M1$	−1.70	0.04	1.50	0.02	0.96

1) Biesecker, D. 2007, the Solar Cycle 24 Prediction Panel, Consensus Statement of the Solar Cycle 24 Prediction Panel, released on March 2007. http://www.swpc.noaa.gov/SolarCycle/SC24/.

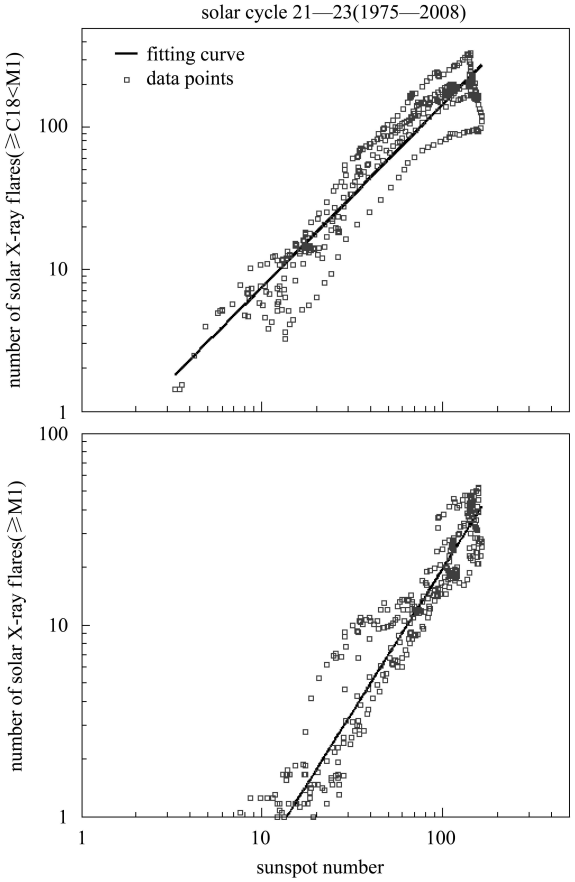

Fig. 4. Scatter plots of the smoothed monthly solar X-ray flare numbers against the sunspot numbers for solar cycles 21—23. (Top panel: flare class $\geqslant C1$ and $< M1$. Bottom panel: flare class $> M1$).

Table 5. The expected monthly numbers of solar X-ray flares in 2011.

X=R_2011	SXR flares $\geqslant C1$ and $< M1$	SXR flares $> M1$
70±10	93±21	12±3
125±20	197±45	28±7

From Tables 3 and 5, we conclude that even if solar cycle 24 is a weak cycle (R_2011=70±10), the mean solar X-ray output in 2011 is expected to exceed 1×10^{-6} W/m^2 (GOES C1-level) and M-flares will occur on average once every 3 days.

4 The expected results of XRS onboard CE-2

4.1 Theoretical lunar X-ray fluorescence production model

The method we used to calculate the anticipated spectra for SXD is based on the theoretical X-ray fluorescence production model described by Clark et al (1997)[3]. In this model, two equations [Eqs. (2) and (3)] are used to determine the intensities of the fluorescent X-ray emission and the scattered X-ray emission respectively from a certain location on the lunar surface.

$$F_{(\mathrm{j})}(\alpha,\beta)=\frac{1}{4\pi}\cdot\omega_{\mathrm{j}}\cdot f_{\mathrm{j}}\cdot\frac{r_{\mathrm{j}}-1}{r_{\mathrm{j}}}\cdot C_{\mathrm{j}}\int\limits_{E_{\mathrm{j,edge}}}\left(\frac{J(E_{\mathrm{c}})\cdot\mu_{\mathrm{j}}(E_{\mathrm{c}})\cdot\mathrm{d}E_{\mathrm{c}}}{\sum\limits_{\mathrm{i}}C_{\mathrm{i}}\left[\mu_{\mathrm{i}}(E_{\mathrm{c}})\sec\alpha+\mu_{\mathrm{i}}(E_{\mathrm{j}})\sec\beta\right]}\right), \tag{2}$$

$$S(E,\alpha,\beta,\theta)=\sum_{\mathrm{i}}\left[\frac{C_{\mathrm{i}}}{A_{\mathrm{i}}}\cdot N_{\mathrm{AV}}\cdot\frac{J(E)\cdot\frac{\mathrm{d}\sigma_{\mathrm{i}}^{\mathrm{coh}}(E,\theta)}{\mathrm{d}\Omega}}{\sum\limits_{\mathrm{i}}C_{\mathrm{i}}\cdot\mu_{\mathrm{i}}(E)\cdot(\sec\alpha+\sec\beta)}\right]+\sum_{\mathrm{i}}\left[\frac{C_{\mathrm{i}}}{A_{\mathrm{i}}}\cdot N_{\mathrm{AV}}\cdot\frac{J(E_{\mathrm{c}})\cdot\frac{\mathrm{d}\sigma_{\mathrm{i}}^{\mathrm{incoh}}(E_{\mathrm{c}},\theta)}{\mathrm{d}\Omega}}{\sum\limits_{\mathrm{i}}C_{\mathrm{i}}\cdot(\mu_{\mathrm{i}}(E_{\mathrm{c}})\sec\alpha+\mu_{\mathrm{i}}(E)\sec\beta)}\right], \tag{3}$$

where i: all elements of the lunar surface, j: elements which emit X-ray fluorescence, μ_{i}: mass attenuation coefficient of i elements, μ_{j}: mass attenuation coefficient of j elements, C_{i}: concentration of i elements, C_{j}: concentration of j elements, ω_{j}: fluorescence yield for j elements, r_{j}: absorption jump ratio for j elements, f_{j}: K-shell electron transfer probability for j elements, E_{j}: energy of j element X-ray fluorescence (Kα and Kβ), E_{c}: energy of primary solar X-rays, E: energy of scattering X-rays, $E=E_{\mathrm{c}}/[1+E_{\mathrm{c}}(1-\cos\theta)/511\ \mathrm{keV}]$, $E_{\mathrm{j,edge}}$: energy of j element K-shell absorption edge, α: incidence angle, β: emission angle, θ: scattering phase angle, N_{AV}: Avogadro number, A_{i}: atomic weight of i elements, $J(E_{\mathrm{c}})$: solar X-ray differential flux, $\frac{\mathrm{d}\sigma_{\mathrm{i}}^{\mathrm{coh}}(E,\theta)}{\mathrm{d}\Omega}$: differential cross-section of i elements for coherent scattering X-rays, $\frac{\mathrm{d}\sigma_{\mathrm{i}}^{\mathrm{incoh}}(E,\theta)}{\mathrm{d}\Omega}$: differential cross-section of i elements for incoherent scattering X-rays, $F_{(\mathrm{j})}(\alpha,\beta)$: intensities of j element X-ray fluorescence ($\mathrm{cm^{-2}\cdot s^{-1}\cdot sr^{-1}}$), $S(E,\alpha,\beta,\theta)$: differential intensities of scattering X-rays ($\mathrm{cm^{-2}\cdot s^{-1}\cdot sr^{-1}\cdot keV^{-1}}$).

In order to calculate the lunar X-ray intensities measured by SXD, $F_{(\mathrm{j})}(\alpha,\beta)$ and $S(E,\alpha,\beta,\theta)$ are integrated over the footprint of SXD, meanwhile, the point spread function and the efficiency[16] of SXD

are also considered in Eqs. (4) and (5).

$$\mathrm{Fluo\_det}_{(\mathrm{j})} = \int\limits_{\mathrm{footprint}} F_{(\mathrm{j})}(\alpha,\beta)\frac{\mathrm{Psf}\cdot\mathrm{Eff}(E_{\mathrm{j}})}{\cos\beta}\mathrm{d}\Omega,$$

$$\mathrm{cm}^{-2}\cdot\mathrm{s}^{-1} \tag{4}$$

$$\mathrm{Scatter\_det}(E) = \int\limits_{\mathrm{footprint}} S(E,\alpha,\beta,\theta)\frac{\mathrm{Psf}\cdot\mathrm{Eff}(E)}{\cos\beta}\mathrm{d}\Omega,$$

$$\mathrm{cm}^{-2}\cdot\mathrm{s}^{-1}\cdot\mathrm{keV}^{-1} \tag{5}$$

where $\mathrm{Fluo\_det}_{(\mathrm{j})}$ is the measured intensity of j element X-ray fluorescence, $\mathrm{Scatter\_det}(E)$ is the measured intensity of scattered X-ray emission, $\mathrm{d}\Omega$ is the differential solid angle of the footprint seen from SXD, Psf is the point spread function of SXD, and $\mathrm{Eff}(E)$ is the detection efficiency of SXD for X-rays with energy E.

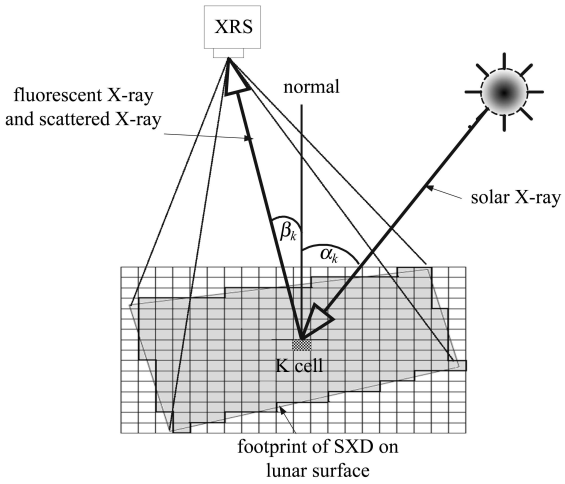

Fig. 5. Lunar X-ray fluorescence production model.

Because the footprint of SXD on the lunar surface is a spherical quadrangle (Fig. 5), direct integration over the footprint in Eqs. (4) and (5) is quite difficult. So, we convert Eqs. (4) and (5) into numerical expressions (Eqs. (6) and (7)) by dividing the footprint into several tens of grid cells (Fig. 5).

$$\mathrm{Fluo\_det}_{(\mathrm{j})} \approx \sum_{k=1}^{N} F_{(\mathrm{j}),k}(\alpha_k,\beta_k)\frac{\mathrm{Psf}_k\cdot\mathrm{Eff}(E_{\mathrm{j}})_k}{\cos\beta_k}\mathrm{d}\Omega_k,$$

$$\mathrm{cm}^{-2}\cdot\mathrm{s}^{-1} \tag{6}$$

$$\mathrm{Scatter\_det}(E)\approx\sum_{k=1}^{N} S_k(E,\alpha_k,\beta_k,\theta_k)\times$$

$$\frac{\mathrm{Psf}_k\cdot\mathrm{Eff}(E)_k}{\cos\beta_k}\mathrm{d}\Omega_k,\quad \mathrm{cm}^{-2}\cdot\mathrm{s}^{-1}\cdot\mathrm{keV}^{-1} \tag{7}$$

where k represents the grid cell which constitutes the footprint and N is the total number of the grid cells in the footprint.

In Eqs. (6) and (7), by summing up the contributions from all the grid cells, we obtain the measured intensities of the fluorescent X-ray emission and the scattered X-ray emission from the entire footprint. Then, the two components of lunar X-rays can be merged into one spectrum. After considering the energy resolution of SXD, we can get the anticipated lunar X-ray spectrum of SXD.

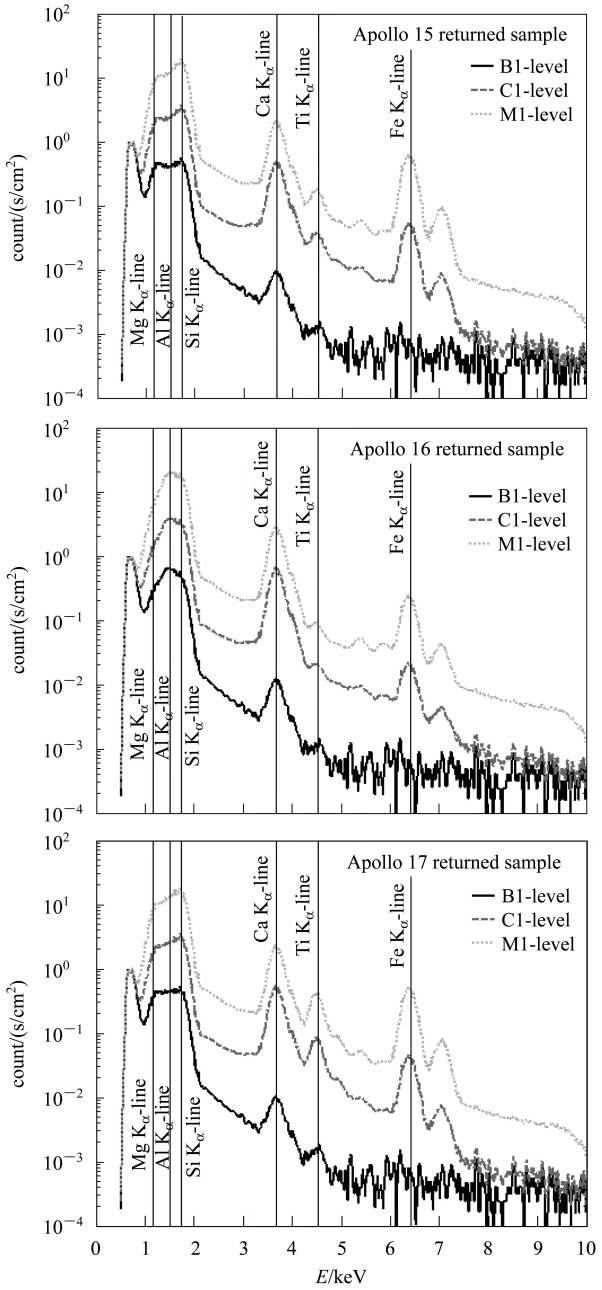

Fig. 6. The simulated XRS (SXD) spectra of different lunar soil samples.

4.2 The anticipated results

The simulated SXD spectra of the Moon's surface are obtained under several assumptions. (1) The observations of SXD are made in a polar circular orbit around the Moon's at an altitude of 100 km and the mean incidence angle of the subpoint is 45 degrees. (2) SXD is a Moon-surface pointing instrument and the satellite platform is three-axis stabilized. (3) Solar X-ray spectra[3] in three levels $B1$, $C1$ and $M1$ are used. (4) Three targets are lunar soil samples returned by Apollo 15, 16, 17 missions respectively[17]. These assumptions represent the typical cases of the observations.

Figure 6 shows the anticipated X-ray spectra calculated for the returned samples. Obviously, the spectral characteristics in Fig. 6 vary with elemental concentration as well as the solar X-ray output level.

Table 6 shows the integration time required to achieve 5σ and 10σ significance for the Kα fluorescent lines of the major elements. Compared with the light elements Mg, Al, Si and Ca, the heavy elements Ti and Fe need much longer integration time. Table 7 shows the anticipated spatial resolution to achieve 5σ significance after 6 months (4320 hours) observation. (As few X-rays are emitted from the night side of the Moon, only 2160 hours' data measured on the day side are used.) From Table 7, we can conclude that if the solar background X-ray level is B1, the spatial resolutions of light elements are several tens of kilometers, while several hundreds of kilometers are achievable for heavy elements Ti and Fe. If the mean solar X-ray output is elevated from B1 to C1, the spatial resolution will be highly improved, especially for the heavy elements. According to the anticipated solar X-ray output in 2011 (see Part 3), C-level condition will prevail through CE-2's mission time and M-flares will occur frequently. As a result, XRS will be able to map the lunar surface with spatial resolutions finer than 100 kilometers for elements Mg, Al, Si, Ca, Ti, and Fe.

Table 6. The integration time required to achieve 5σ and 10σ significant level for the major rock-forming elements.

element		Apollo15 sample		Apollo16 sample		Apollo17 sample	
		$B1$	$C1$	$B1$	$C1$	$B1$	$C1$
Mg	5σ	13s	2s	43s	6s	16s	2s
	10σ	52s	7s	171s	24s	62s	8s
Al	5σ	17s	3s	5s	1s	12s	2s
	10σ	66s	11s	18s	3s	47s	8s
Si	5σ	5s	1s	6s	1s	45s	1s
	10σ	17s	2s	22s	3s	19s	2s
Ca	5σ	5.4min	3s	3.2min	2s	4.6min	2s
	10σ	21.5min	10s	12.8min	7s	18.4min	9s
Ti	5σ	2.9d	2.4min	19.0d	13.8min	8.5h	25s
	10σ	11.5d	9.4min	75.9d	55.4min	1.4d	1.7min
Fe	5σ	1.1d	29s	7.4d	2min	1.6d	39s
	10σ	4.4d	2.0min	29.7d	8.2min	6.3d	2.6min

Note: Time: d, days; h, hours; min, minutes; s, seconds.

Table 7. The anticipated spatial resolution (Y) to achieve 5σ significance for the major lunar elements.

element	Apollo15 sample		Apollo16 sample		Apollo17 sample	
	$B1$	$C1$	$B1$	$C1$	$B1$	$C1$
Mg	35	22	47	29	37	22
Al	37	24	27	18	34	22
Si	27	18	29	18	48	18
Ca	78	24	68	22	75	22
Ti	411	64	657	98	243	41
Fe	322	43	519	61	354	46

Note: Spatial resolution is also represented by $Y \times Y$ square of kilometers.

5 Conclusion

The above calculations indicate that the upcoming solar maximum in 2011 will afford a golden opportunity for XRS onboard CE-2 to measure the elemental compositions of the lunar surface. The magnitude of the solar background X-ray flux will be higher than C1-level, and the anticipated spatial resolutions of several tens of kilometers can be achieved for the distributions of the six major rock-forming elements (Mg, Al, Si, Ca, Ti, and Fe), which will provide detailed information to understand the geochemical nature of terrains and to establish a lunar resource distribution database for future exploration and utilization.

References

1 Adler I, Gerard J, Trombka J I et al. The Apollo 15 X-ray Fluorescence Experiment. Proc. Lunar Sci. Conf. 3rd, 1972. 2157—2178
2 Adler I, Trombka J I. Naturwissenschaften, 1973, **60**(5): 231—242
3 Clark P E, Trombka. J. Geophys. Res. E, 1997, **102**(7): 16361—16384
4 Truscott P, Dyer C, Peerless C. Basalt X-ray Fluorescence Study, basalt study Issue 0.b, DERA Space Depart. for ESA/ESTEC, 2000
5 Bouwer S D. J. Geophys. Res. A, 1983, **88**(10): 7823—7830
6 WANG Huan-Yu, ZHANG Cheng-Mo et al. Nuclear Electronics & Detection Technology, 2008, **28**(2): 215—218 (in Chinese)
7 OUYANG Zi-Yuan, JIANG Jing-Shan, LI Chun-Lai et al. Chin. J. Space Sci, 2008, **28**(5): 361—369
8 SUN Hui-Xian, WU Ji, DAI Shu-Wu et al. Chin. J. Space Sci., 2008, **28**(5): 374—384
9 Hathaway D H, Wilson R M. Geophys. Res. Lett., 2006, **33**: L18101
10 Hathaway D H. Space Sci. Rev., 2008.9 (online first), DOI: 10.1007/s11214-008-9430-4
11 Veronig A M, Temmer M. Arnold Hanslmeier. Solar Physics, 2004, **219**: 125—133
12 Hathaway D H, Wilson R M, Reichmann E J. J. Geophys. Res. A, 1999, **104**(10): 22375—22388
13 Gough D. Nature, 2001, **410**: 313—314
14 Babcock H W. Astrophys. J., 1961, **133**(2): 572—587
15 Pesnell W D. Solar Physics, 2008, **252**: 209—220
16 ZHANG Jia-Yu, WANG Huan-Yu, ZHANG Cheng-Mo et al. Nuclear Electronics & Detection Technology, 2007, **27**(4): 651—653 (in Chinese)
17 McKay D et al. The Lunar Regolith. In: Heiken G H, Vaniman D T, French B M (Editors), Lunar Sourcebook: A User's Guide to the Moon. New York: Cambridge Univ. Press, 1991. 346